ELSEVIER

Journal of Marine Systems 25 (2000) 405–419

JOURNAL OF MARINE SYSTEMS

www.elsevier.nl/locate/jmarsys

Towards a 3D-ecosystem model of the Baltic Sea

Thomas Neumann *

Baltic Sea Research Institute, Seestrasse 15, 18119 Warnemünde, Germany

Received 16 March 1999; accepted 17 August 1999

Abstract

The paper describes briefly the preliminary results of a coupled chemical–biological and circulation model of the Baltic Sea. The chemical–biological model involves nine state variables to simulate the nitrogen cycle. A 1-year simulation shows how the model could be used to estimate budgets and nitrogen transports. The importance of shallow coastal areas for the removal of riverborne nitrogen is demonstrated on the Pomeranian Bight area. Within the simulation period, only 15% of the Oder river nitrogen load have left the Pomeranian Bight into the Baltic Sea. © 2000 Elsevier Science B.V. All rights reserved.

Keywords: Baltic Sea; ecosystem; modelling; nitrogen cycle

1. Introduction

The Baltic is a semi-enclosed, brackish water sea, which consists of several basins of different depth. The positive water balance of the Baltic, due to fresh water surplus, and the reduced water exchange with the North Sea through the narrow and shallow connecting channels, imply an estuarine general circulation with a well pronounced vertical density stratification. The deep basins of the Baltic are partly under anoxic conditions which are interrupted after the so-called major salt water inflows (Rheinheimer, 1996).

Developed industrial countries with intensive agriculture surround the Baltic. River runoff and atmospheric input to the Baltic have anthropogenic-increased loads of nutrients. An increase or decrease of nutrient input may alter the productivity of the system, and in turn, the oxygen conditions in the deep parts of the Baltic. The ecosystem of the Baltic is influenced by changing redox conditions with depth and time. Key questions are: How does the ecosystem react to altered boundary conditions? What are the pathways of nutrients? Which measures could be applied to recover from anthropogenic impact? These problems have been studied in several papers (see e.g., Stigebrandt and Wulff, 1987).

To answer these questions requires a sound quantitative understanding of the processes by combining observations and models. Recently, the use of numerical models, which integrate circulation and biology, became of increasing importance. Nowadays, available compute power enable an efficient way to run high resolving physical models coupled with bio-chemical models. In the recent paper, first results of a coupled physical–bio-chemical model of the Baltic Sea are presented with focus on the application to support nitrogen budget estimates. One main

* Tel.: +49-381-52970; fax: +49-381-5197-440.

E-mail address: thomas.neuman@io-warnemuende.de (T. Neumann).

0924-7963/00/$ - see front matter
PII: S0924-7963(00)00030-0

objective of the model development and application is the simulation of nitrogen fluxes, both the propagation through the food web and the physical transport. The model is considered to be an important step towards an ecosystem model of the Baltic Sea. In the recent paper, we have considered the nitrogen budget in a coastal area.

2. The circulation model

The circulation model is based on the Modular Ocean Model MOM2.2 (Pacanowski et al., 1990) with an implementation of an explicit free surface. The model covers the Baltic Sea with a total area of 0.443×10^{12} m^2 and a total volume of 0.244×10^{14} m^3. The horizontal resolution is 3 nautical miles and the vertical resolution is 2 m for the first 12 layers and increasing with depth. An open boundary condition at the western border of the Skagerrak with prescribed sea levels and salinity is applied (Mutzke, 1998). To provide riverine freshwater runoff and nutrient input, the 15 largest rivers are included. An atmospheric boundary layer model derives the ocean surface fluxes from the meteorological forcing data.

The horizontal turbulent viscosity and diffusivity are estimated by the Smagorinski (Rosati and Miyakoda, 1988) nonlinear mixing scheme, whereas for the vertical mixing, the Richardson-number model of Pacanowski and Philander (1981) is used. Both are implemented as standard options in the MOM2.

This model type has been successfully applied to the Baltic Sea in Lehmann (1995). In Fennel and Neumann (1996, 1999), the MOM code was used as hydrodynamical base for a test bed model of the western Baltic Sea to analyse a chemical–biological model. Siegel et al. (1998) demonstrate the application of MOM2.2 coupled to a chemical–biological model to investigate the fate of the Oder flood event.

3. The chemical–biological model

The chemical–biological model simulates a nitrogen cycle. The basic formulations are described in Fennel (1995), Fennel and Neumann (1996), as well as in Stigebrandt and Wulff (1987). Compared to the model in Fennel and Neumann (1996), additional processes, such as denitrification and nitrogen fixation, are involved in order to carry out longer model runs. Most of the model parameters are taken from literature and refined by tuning the model in a one-dimensional case. As expected, the most sensitive parameter is the phytoplankton uptake rate. It influences the timing of phytoplankton blooms. Parameters for blue-green algae group dynamics were chosen following Wasmund (1997).

A conceptual sketch of the model is shown in Fig. 1. Primary producers are divided into three functional groups called diatoms, flagellates and blue-green algae. The diatoms group represents large phytoplankton, the flagellates group, smaller phytoplankton and the blue-green algae group provides nitrogen fixation. The primary production is driven by solar radiation and uptake of nitrogen. Whereas the diatoms and flagellates use dissolved nitrate and ammonium, the blue-green algae group is able to take up atmospheric nitrogen and, hence, this group acts as a nitrogen source for the system. Different physiological parameters allow different ecological optima for the algae groups depending on available nutrient concentrations, temperature and sinking velocity (Eqs. B11–13). The diatoms dominate new production and the flagellates dominate regenerated production. Under low nitrate and ammonium concentrations, blue-green algae get an advantage and could become dominating.

Grazing converts the phytoplankton nitrogen into zooplankton and mortality of phytoplankton and zooplankton controls the nitrogen flux into detritus. The recycling process of detritus to nutrients provides an ammonium flux. Depending on oxygen conditions, ammonium is nitrified to nitrate. Phosphate is included to limit the blue-green algaes' growth and is coupled to nitrogen via the Redfield ratio.

In the model, the oxygen demand and production of oxygen is coupled to nitrogen conversion. The oxygen concentration controls the recycling of dead organic matter (detritus). If the oxygen is depleted, then the nitrate is used to oxidize detritus and, if nitrate disappears, sulphate is reduced to hydrogen sulphide. Hydrogen sulphide is accounted for by negative oxygen equivalents. Reduction of nitrate (denitrification) is counted as a loss of nitrogen in the model.

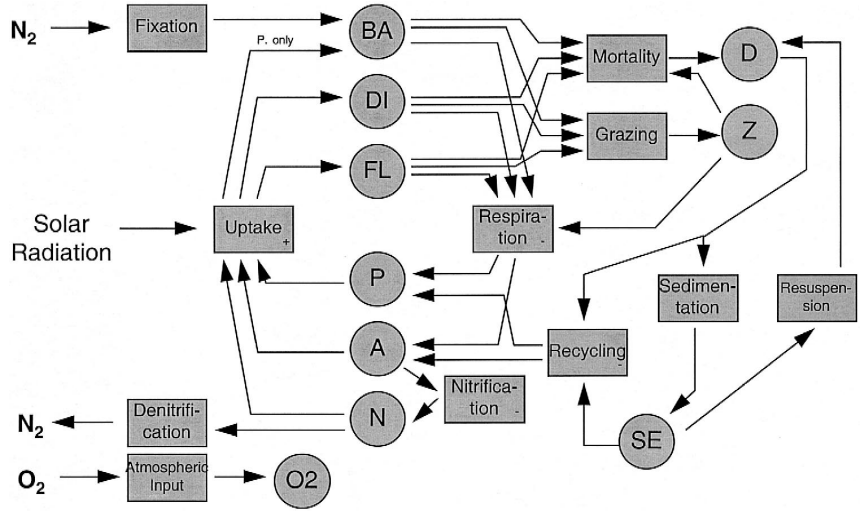

Fig. 1. Conceptual chemical–biological model. Circles are for state variables and rectangles for processes, respectively. In detail, state variables are: ammonium (A), nitrate (N) phosphate (P), flagellates (FL), diatoms (DI), blue-green algae (BA), detritus (D), zooplankton (Z), oxygen (O2) and sediment (SE).

At the bottom, we introduce an additional sediment layer, where sinking detritus accumulates. Suspension and resuspension of detritus is taken into account and occurs if the currents near the bottom exceed critical values. In sediment layer, the detritus can be mineralized and may be released as ammonium. Denitrification of 50% of the mineralized nitrogen occurs within the sediments around a hypothetical redoxcline if the water above the sediments is oxic (RECSN in Eq. B8). For phosphorus, the sediment is a sink simulating the absorption onto solid particles (iron-III complexes) under oxic conditions. The chemical–biological model code is embedded as a module in the circulation model and coupled via the advection–diffusion equation.

4. Model setup and forcing

The simulation period was from October 1996 until October 1997. The model is forced with meteorological data from the HIRLAM weather forecast model. Meteorological analysis data for that period were used as forcing data. Initial fields for temperature and salinity were obtained from climatological data sets (Bock, 1971; Lenz, 1971). Initializing the chemical–biological model, data from previous runs, as well as from measurements, were used. The initial load of total nitrogen in the water column is 1613 kt, which responds to a concentration of about 4.5 mmol N m^{-3}. In sediments, a total nitrogen load of about 804 kt was initialised. Atmospheric input of nutrients were obtained from Helcom (1994). Climatological, riverborne freshwater runoff data from Bergström and Carlsson (1994) and Mikulski (1970) drive freshwater and data from Rheinheimer (1996) nutrient input. We have to note that the runoff data, as well as the atmospheric input data, are climatological data. From that point, the intension was not to reproduce the period October 1996 until October 1997. In fact, the general model behaviour was analysed with emphasis on the nitrogen budget.

5. Baltic Sea nitrogen budgets

In order to obtain a general impression of the model performance, we first look at the simulated global Baltic nitrogen budget. The changes in nitrogen inventory, as well as nitrogen fluxes within the modelled period, are shown in Table 1. Negative or positive values represent losses or gains, respectively. In the water column, the model simulates a loss of about 44 kt total nitrogen which corresponds to a decrease of 0.13 (mmol N_{tot}) m^{-3}. Stigebrandt and Wulff (1987) have estimated year-to-year variations of ∓ 90 kt total nitrogen which is in the same order. The numbers for the atmospheric and river-

Table 1
Modelled Baltic Sea nitrogen budget (Nov. 96–Oct. 97)

	Nitrogen (kt)
Total N in water column	−44.18
Total N in sediments	215.14
Riverborne input	513.56
Atmospheric input	275.00
Lateral transports to North Sea	−22.70
Denitrification in water column and sediments	−608.04
N fixation	13.14

borne inputs are derived from forcing data. The modelled denitrification losses and accumulation in sediments compare well with the values given in Stigebrandt and Wulff (1987) and Losán et al. (1996). However, the nitrogen fixation due to blue-green algae gives comparable small values (see also Fig. 4).

6. Spring bloom delay

A well-known phenomenon of the southern Baltic Sea is the delayed spring bloom from west to east (see Kayser and Schulz, 1976; Fennel and Neumann, 1999). This behaviour is also found in model, as visible in Fig. 2, which shows the mean chlorophyll *a* values from the Baltic Sea basins Belt Sea and Mecklenburg Bight, Arkona Sea and Bornholm Sea. Between the peak of the blooms, one finds a time delay of about 2 weeks. The delay is consistent with the Sverdrup criteria. Regions with deeper mixed layer bounded by the halocline require more heat to establish a thermal stratification if water is cooled below the density maximum (see Fennel and Neumann, 1999). Another view at the spring bloom delay is provided in Fig. 3. It shows the surface chlorophyll *a* patterns at three different dates. Around March 25th, the bloom starts in Kategatt and Belt Sea with increased concentrations. Apart from the vicinity of river mouths, the algaes' biomass remains at low level. At April 9th, the Arkona Sea is covered by high phytoplankton concentrations, and later on, at April 29th, the Bornholm Sea and western parts of Baltic Proper show the growing phytoplankton concentrations. The bloom apparently starts in shallow coastal areas and spread into deeper parts of the basins.

7. Succession of plankton species

The successions of the different model phytoplankton groups during the course of a year is as expected. Diatoms dominate the spring bloom, flagellates grow up later and dominate in summer. Depleted nitrogen and high temperature favour blue-green algae (Wasmund, 1997). Late blooms in autumn are dominated by both diatoms and flagellates and depend on available nutrients. Two examples are shown in Fig. 4, where the mean chlorophyll *a* concentration for the distinct phytoplankton groups is displayed for two different model areas. Fig. 4a is from the Gotland Basin with relatively low nutrient concentrations. Diatoms dominate the spring bloom, whereas flagellates dominate in summer and autumn. In late summer, the peak of blue-green algaes occurs. In contrast, Fig. 4b shows, an area with high nutrient loads, the Pomeranian Bight. It is only in summer that flagellates are more abundant than diatoms. Blue-green algae plays a minor role for the total biomass. Thus, we can conclude that the model simulates the succession of competing algae groups depending on environmental conditions in a reasonable manner.

8. Oxygen depletion

Oxygen is an important environmental parameter for the Baltic Sea, as well as a key parameter for the modification of the nitrogen fluxes. The model simu-

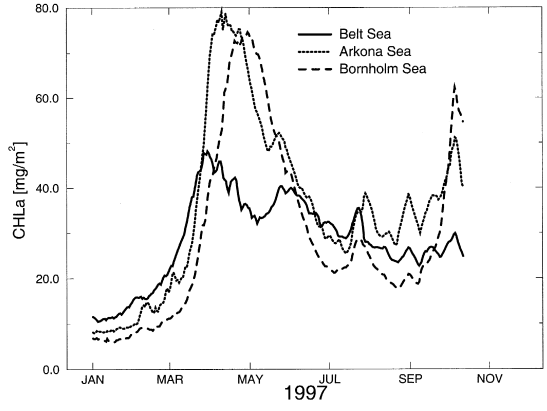

Fig. 2. Mean chlorophyll *a* in different model regions. Between the peaks of spring bloom is a time delay of about 2 weeks.

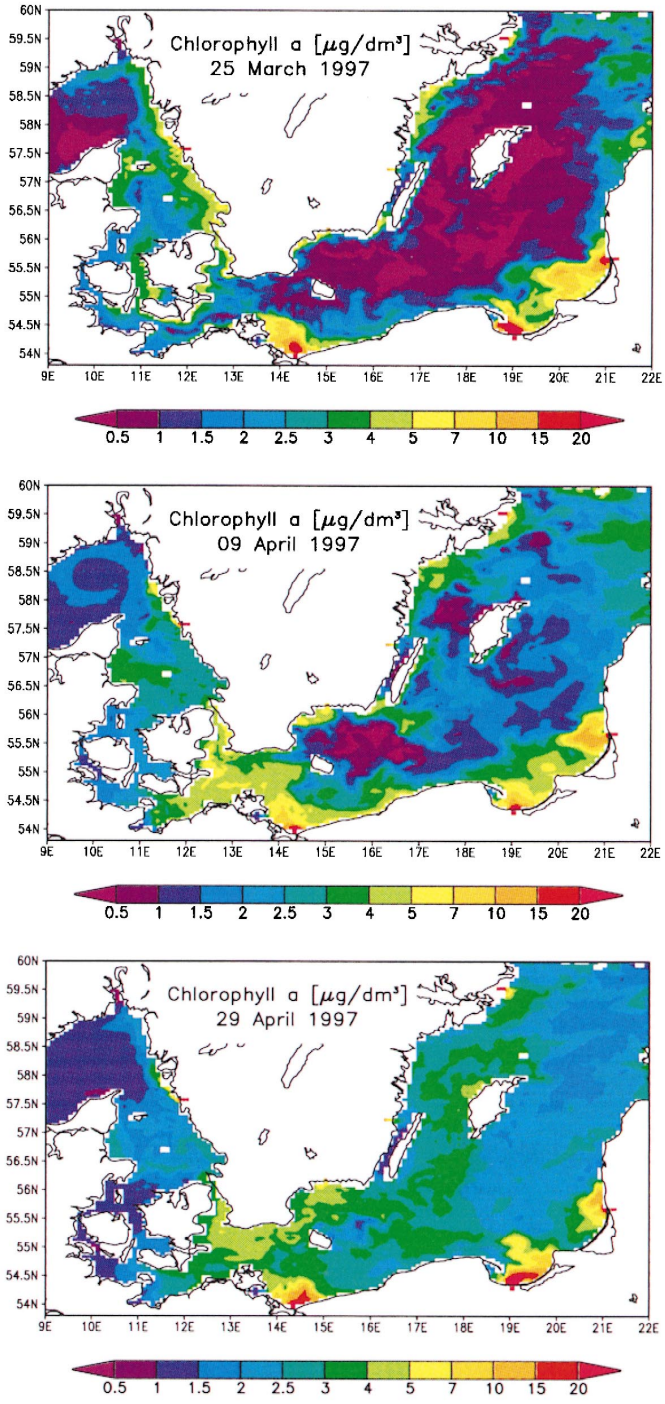

Fig. 3. Modelled surface chlorophyll *a* concentration.

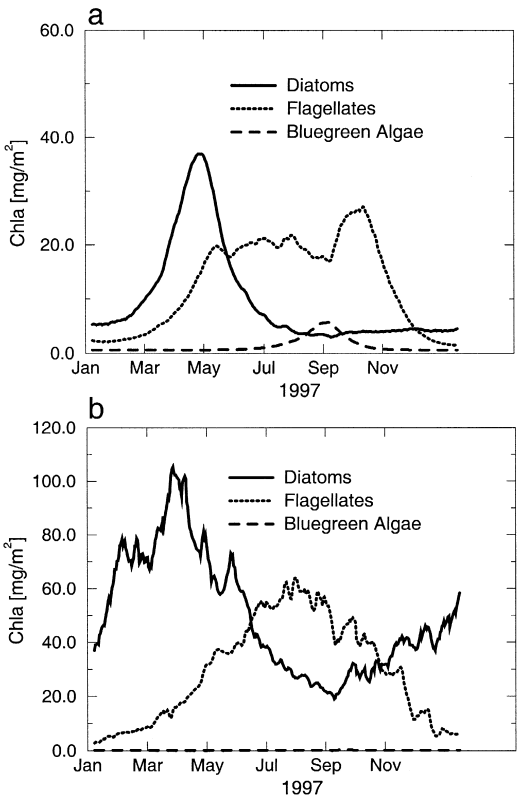

Fig. 4. Annual cycle of three model algae groups in Baltic Proper (a) and Pomeranian Bight (b).

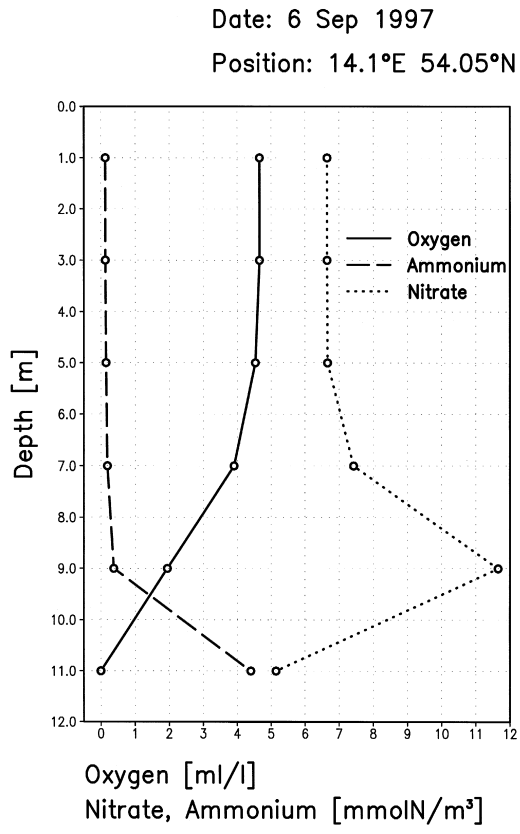

Fig. 5. Vertical profile taken from a model station in the Pomeranian Bight.

lates oxygen concentration, which in turn controls the processes of denitrification and nitrification. To illustrate how the oxygen influences the nitrogen cycle, we show in Fig. 5 a vertical profile of oxygen, ammonium and nitrate at a shallow water station in the Pomeranian Bight in late summer. The oxygen concentration is depleted close to the bottom. This implies that nitrate is used to oxidize organic matter and the result is a reduced nitrate concentration. Recycled ammonium cannot be oxidized (no nitrification) and, hence, the concentration of ammonium increases.

In the model run under consideration, the oxygen concentration was not completely depleted in deep basins. This is due to the relatively high initial concentrations. However, the mean deep water oxygen concentration in the Baltic Proper is continuously decreasing over the model period as seen in Fig. 6. From the processes wherein the deep water in the central basin are shown, we can expect that the spin-up of the coupled model has not been finished after a year time for deep areas.

The pattern of the oxygen concentrations close to the bottom is shown in Fig. 7. After a calm weather

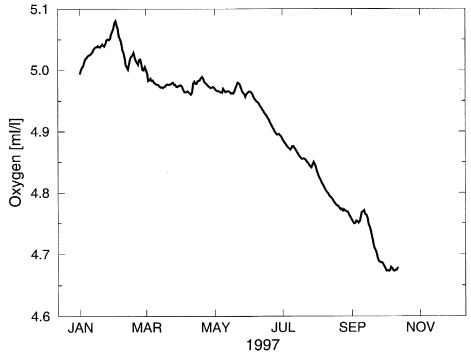

Fig. 6. Mean model oxygen in Baltic Proper below 110 m depth.

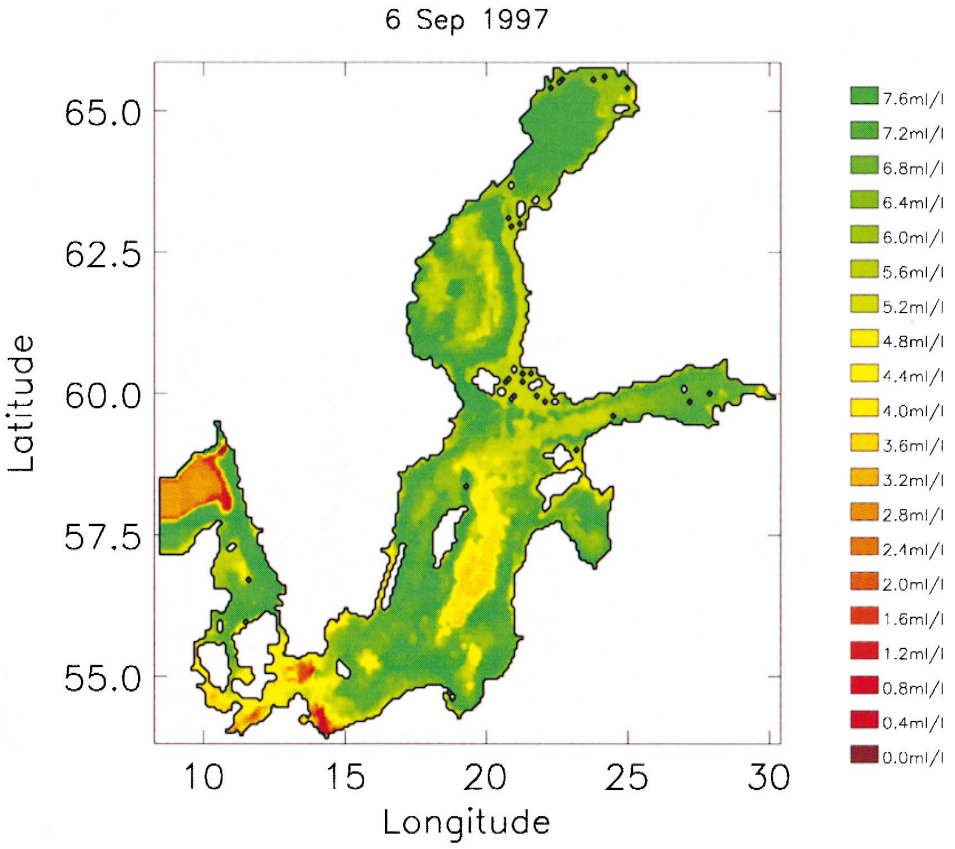

Fig. 7. Model oxygen in the nearest bottom layer.

period in August 1997, we find in shallow areas the typical low oxygen regions in Lübeck Bight, Arkona Sea and Pomeranian Bight. Weak mixing due to low wind speeds, strong thermal stratification and high organic loads have supported a fast decrease of the oxygen content. Field observations in Pomeranian Bight in late August 1997 (see Siegel et al., 1998) confirm the occurrence of zero values of oxygen concentration and the occurrence of hydrogen sulphide.

9. Coastal zone budget — Oder estuary

In order to demonstrate the capability of the model to simulate fluxes of matter, we look at nitrogen transports in a coastal area. We consider, in particular, the Pomeranian Bight, which is sur-

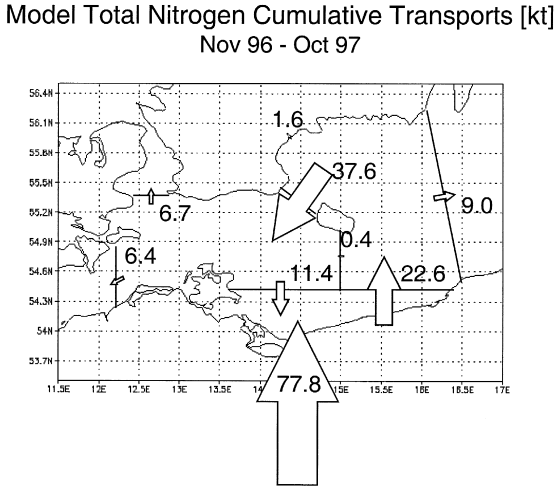

Fig. 8. Cumulative lateral model transports of total model nitrogen.

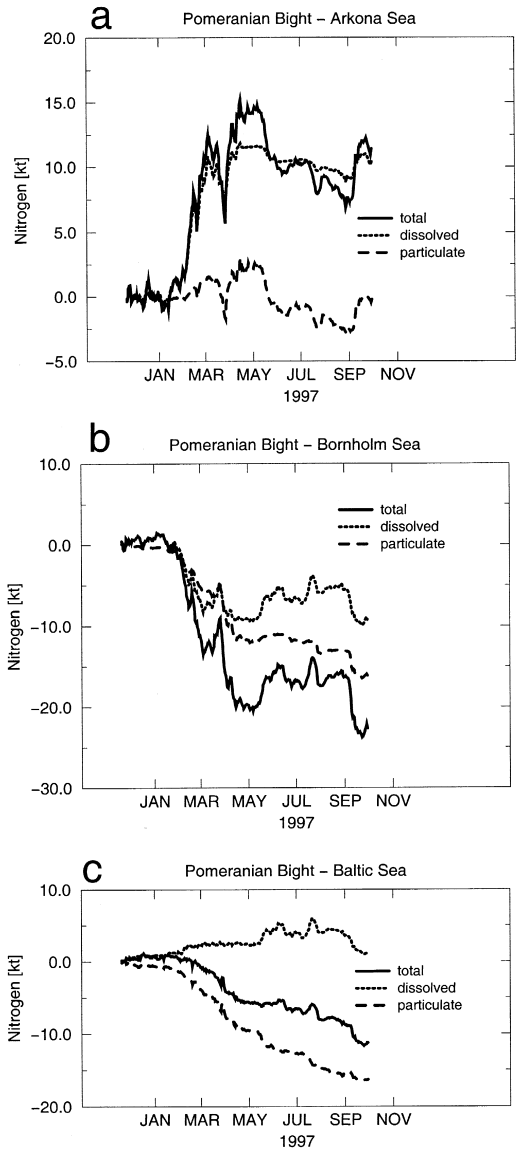

Fig. 9. Annual cycle of cumulative total model nitrogen transports across a section separating Pomeranian Bight and Arkona Sea (a), Pomeranian Bight and Bornholm Sea (b) and the sum of both (c).

rounded by the Arkona and Bornholm Sea. The Pomeranian Bight is the shallow, estuarine region of the Oder river. Most parts of the bottom are sandy. This means the bight is more a transit than an accumulation area. Hence, the nitrogen load from the Oder river estuary will be transported into the deeper basins or removed by denitrification.

To discuss the net fluxes of total nitrogen from the Oder mouth down to the central basins, we divided the model area into several regions. The cumulative transports of total nitrogen across the boundaries are shown in Fig. 8. The total nitrogen input of the Oder river is about 78 kt. From the Arkona Sea into the Pomeranian Bight, the model estimates a net input of about 11.4 kt total nitrogen and a net export of about 22.6 kt total nitrogen into the Bornholm Sea. Cumulative transports across the southern boundary between Arkon and Bornholm Sea are very low (0.4 kt nitrogen) because transports are concentrated on the coast within coastal jets and crossing the Pomeranian Bight.

A more detailed view into transports gives Fig. 9 where negative and positive transports describe nitrogen losses and gains, respectively. In Fig. 9a, the cumulative transports between Pomeranian Bight and Arkona Sea are shown. The transport of total nitrogen is split into the flux of particulate nitrogen accumulated in algae and detritus and dissolved nitrogen. Obviously, the total transport is dominated by dissolved nitrogen. A substantial amount of nitrogen has entered the Pomeranian Bight in spring, whereas in summer, only marginal net transports occur. However, in summer, a more or less continuous transport of particles into the Arkona Sea is simulated. In spring, the transports into Bornholm Sea (Fig. 9b) of both parts particulate and dissolved

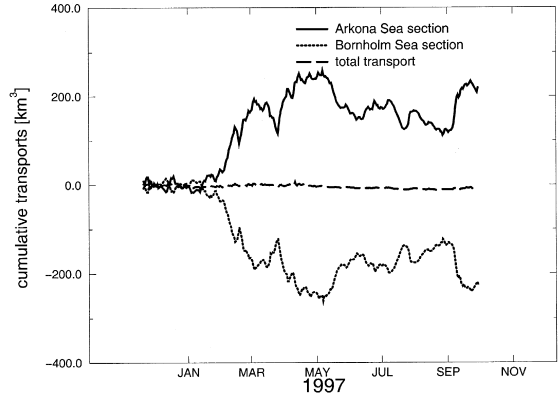

Fig. 10. Annual cycle of cumulative volume transports across a section separating Pomeranian Bight and Arkona Sea (solid line), Pomeranian Bight and Bornholm Sea (dotted line) and the sum of both (dashed line).

Table 2
Modelled Pomeranian Bight nitrogen budget (Nov. 96–Oct. 97)

	Nitrogen (kt)
Total N in water column	3.70
Total N in sediments	14.94
Riverborne input	77.84
Atmospheric input	8.42
Lateral transports to Baltic	−11.24
Denitrification in water column and sediments	−56.39
N fixation	0.01

are nearly the same. During summer, particles are exported and dissolved nitrogen is imported. The resulting transport into the Baltic (Fig. 9c), i.e. the net export to the Arkona and Bornholm Sea, is dominated by particles. Fig. 10 displays the cumulative volume transports across both sections separating the Pomeranian Bight from the Baltic Sea. It becomes obvious that the transports of nitrogen are strongly related to the volume transports. The total transport is about 10 km^3 and reflects the Oder freshwater runoff.

The model simulation allowed budget estimates. The difference of total nitrogen in the water column and sediments and the riverborne and atmospheric inputs and transports across the vertical section, together with denitrification and nitrogen fixation values close the budget. The nitrogen fixation in the Pomeranian Bight is negligible, as seen from Fig. 4, and the denitrification in the water column plays only a minor role. The loss of about 56 kt nitrogen is mainly due to denitrification in the sediments and corresponds to a rate of about 0.633 $mol/(m^2\ a)$. The modelled components of the budget of the Pomeranian Bight are listed in Table 2.

In the model run, the Pomeranian Bight displays an effective region to remove riverborne nitrogen. As seen from Table 2, an amount of 56 kt nitrogen, i.e. 65% of riverine and atmospheric input have been removed from the system within the Pomeranian Bight.

10. Summary

The annual cycle of nitrogen in the Baltic Sea was simulated with a high spatial resolution coupled model and first results are discussed. The involved physiological parameters of the phytoplankton groups in conjunction with the physical forcing control a succession of model species. The timing of the occurrence of phytoplankton depends on the annual meteorological cycle and the responses of the sea (vertical stratification and currents), as well as on regional particularity, such as availability of nutrients. This is important in harmful algae bloom studies or in simulation of pray fields for higher trophic levels.

Simulated nitrogen budget for the Pomeranian Bight shows the importance of shallow coastal areas for nitrogen removal from the Baltic Sea. Only 11.2 kt nitrogen or about 13% of inputs have left this area to enter deeper basins. The fate of exported nitrogen is strongly connected to weather conditions, which determine whether nitrogen is transported into Arkona or Bornholm Sea. A net export from the Pomeranian Bight was observed only for particulate nitrogen.

The nitrogen budget for the whole Baltic Sea may be affected by the initial conditions. In the coastal zone area, this effect vanishes within a few weeks of model time because of the short residence time and the high nitrogen throughput in the Pomeranian Bight.

Acknowledgements

The author would like to thank his colleagues of the Baltic Sea Research Institutes modelling group who support the circulation model. Further, I would like to thank three anonymous referees for numerous helpful hints. The investigations were partly supported by the project ERGOM of the Bundesministerium für Forschung und Technologie (project number: 03F0230A).

Appendix A. Nomenclature

All state variables are normalised and, hence, are dimensionless. They could be rescaled by multiplying with Nnorm for nitrogen variables and with Onorm for oxygen, respectively. Subscript n, used in phytoplankton-related variables, refers to the different functional algae groups with $n = 1$ the diatoms group, $n = 2$ the flagellates group and $n = 3$ the blue-green algae group.

Symbol	Meaning	Unit
A	state variable NH_4 (ammonium)	
AFLX	NH_4 surface flux	m/day
α_1	half-saturation diatoms	
α_2	half-saturation flagellates	
α_3	half-saturation blue-greens	
D	state variable detritus	
DN	constant scaling mineralisation of detritus	day^{-1}
DS	constant scaling mineralisation of sediment	day^{-1}
e	Euler constant (2.71828...)	
G	zooplankton grazing	day^{-1}
G_0	zooplankton grazing constant	day^{-1}
G_n	zooplankton grazing on phytoplankton n	day^{-1}
H	model surface layer thickness	m
H_{BOT}	layer thickness close to bottom	m
I	illuminance	W/m^2
IV	Ivlev constant	
I_{min}	minimum PAR	
I_{opt}	illuminance optimum for photosynthesis	W/m^2
I_0	solar radiation at the sea surface	W/m^2
k_w	attenuation constant sea water	m^{-1}
k_c	attenuation constant self shading	$m^2/mmol$
LP	loss of phytoplankton	day^{-1}
LPD	loss of phytoplankton to detritus	day^{-1}
LPN	loss of phytoplankton to NH_4	day^{-1}
LZ	loss of zooplankton	day^{-1}
LZD	loss of zooplankton to detritus; including mortality, fecal pellets, ingestion loss	day^{-1}
LZN	loss of zooplankton to NH_4	day^{-1}
N	state variable nitrate	
NI0	nitrification constant	day^{-1}
NF	nitrification rate	day^{-1}
NFLX	nitrate surface flux	m/day
$NLIM_n$	nitrogen limitation	
Nnorm	non-dimensionalisation constant for nitrogen	$mmol/m^3$
O2	state variable oxygen	
O_{hsn}	constant scaling the oxygen dependence of nitrification	
OFLX	oxygen surface flux	m/day
Onorm	non-dimensionalisation constant for oxygen	$mmol/m^3$
P_n	state variable algae groups	
PAR	photosynthetically active radiation	W/m^2
POFLX	phosphate surface flux	m/day
$PLIM_n$	phosphate limitation	
PO	state variable phosphate	
PPI	light limitation (PI curve)	
PV	piston velocity	m/day
R_n	uptake rate	day^{-1}
RA_n	uptake rate ammonium	day^{-1}
REC	mineralisation rate of detritus	day^{-1}

RECS	mineralisation rate of organic matter in sediments	day^{-1}
RECSN	part of mineralized nitrogen in sediments which in turn is nitrified and denitrified	day^{-1}
RES	resuspension rate	day^{-1}
RFR	Redfield ratio	N/P
RN_n	uptake rate nitrate	day^{-1}
SED	state variable sediment	
SEDR	sedimentation rate	m/d
T	temperature	°C
T_{hsr}	constant scaling temperature dependence of detritus mineralisation	°C
Ths_n	constant scaling temperature dependence of phytoplankton uptake	°C
T_{optz}	temperature optimum of zooplankton grazing	°C
T_{scd}	constant scaling the temperature effect on detritus mineralisation	
T_{scn}	constant scaling the temperature effect on nitrification	$°C^{-1}$
T_{scs}	constant scaling the temperature effect on sediment mineralisation	$°C^{-1}$
$TLIM_n$	temperature dependence of phytoplankton uptake	
TLIMN	temperature dependence of nitrification	
TLIMZ	temperature dependence of zooplankton grazing	
Z	state variable zooplankton	

Appendix B. Model equations

B.1. Model dynamics

Terms concerning surface fluxes are taken into account only in the model surface layer whereas terms describing fluxes between water column and sediment are taken into account only in the model layer close to bottom.

$$\dot{A} = -\sum_{n=1}^{2} RA_n P_n + REC \cdot D + \frac{RECS}{H_{BOT}} SED + LPN \sum_{n=1}^{3} P_n + LZN \cdot Z^2 - NF \cdot A + \frac{AFLX}{H} \quad (B1)$$

$$\dot{N} = -\sum_{n=1}^{2} RN_n P_n + NF \cdot A - 5.3\left(REC \cdot D + \frac{RECS}{H_{BOT}} SED\right) \times (1 - OSWTCH) NSWTCH + \frac{NFLX}{H} \quad (B2)$$

$$\dot{PO} = RFR\left[REC \cdot D + LPN \sum_{n=1}^{3} P_n + LZN \cdot Z^2 - \sum_{n=1}^{3} R_n P_n\right] + \frac{POFLX}{H} \quad (B3)$$

$$\dot{P}_n = R_n P_n - LP \cdot P_n - G_n Z; \qquad \{n = 1,2,3\} \quad (B4)$$

$$\dot{Z} = G \cdot Z - LZ \cdot Z^2 \quad (B5)$$

$$\dot{D} = LPD \sum_{n=1}^{n} P_n + LZD \cdot Z^2 - (REC + SEDR) D + RES \cdot SED \quad (B6)$$

$$\dot{O2} = \frac{Nnorm}{Onorm}\left[\frac{6.625 \cdot A + 8.125 \cdot N}{A + N} \sum_{n=1}^{3} R_n P_n - 1.5 \cdot NF \cdot A - 6.625\left(LPN \sum_{n=1}^{3} P_n + LZN \cdot Z\right) - 6.625\left(REC \cdot D + \frac{RECS}{H_{BOT}} SED\right)(NSWTCH \cdot OSWTCH\right.$$

$$+(1-\mathrm{NSWTCH}))\Bigg] - 1.5\cdot\frac{\mathrm{RECSN}}{H_{\mathrm{BOT}}} \times \mathrm{SED}\cdot\mathrm{OSWTCH} + \frac{\mathrm{OFLX}}{H} \quad \text{(B7)}$$

$$\dot{\mathrm{SED}} = \mathrm{SEDR}\cdot\mathrm{D} - (\mathrm{RES}+\mathrm{RECS})\cdot\mathrm{SED} - \mathrm{RECSN}\cdot\mathrm{SED} \quad \text{(B8)}$$

B.2. Rates

B.2.1. Phytoplankton rates

$$\mathrm{RA}_n = \frac{\mathrm{A}}{\mathrm{A}+\mathrm{N}}R_n \quad \text{(B9)}$$

$$\mathrm{RN}_n = \frac{\mathrm{N}}{\mathrm{A}+\mathrm{N}}R_n; \qquad \{n=1,2,3\} \quad \text{(B10)}$$

$$R_1 = R\mathrm{D0}\cdot\min(\mathrm{NLIM}_1,\mathrm{PLIM}_1,\mathrm{PPI}); \quad \text{diatoms} \quad \text{(B11)}$$

$$R_2 = R\mathrm{F0}\cdot\mathrm{TLIM}_2\cdot\min(\mathrm{NLIM}_2,\mathrm{PLIM}_2,\mathrm{PPI}); \quad \text{flagellates} \quad \text{(B12)}$$

$$R_3 = R\mathrm{B0}\cdot\mathrm{TLIM}_3\cdot\min(\mathrm{PLIM}_3,\mathrm{PPI}); \quad \text{blue-greens} \quad \text{(B13)}$$

$$\mathrm{NLIM}_n = \frac{(\mathrm{A}+\mathrm{N})^2}{\alpha_n+(\mathrm{A}+\mathrm{N})^2} \quad \text{(B14)}$$

$$\mathrm{PLIM}_n = \frac{\mathrm{PO}^2}{\mathrm{RFR}\cdot\alpha_n+\mathrm{PO}^2} \quad \text{(B15)}$$

$$\mathrm{TLIM}_2 = 1+\frac{T^2}{\mathrm{Ths}_2^2+T^2} \quad \text{(B16)}$$

$$\mathrm{TLIM}_3 = \frac{1}{1+\exp(\mathrm{Ths}_3-T)} \quad \text{(B17)}$$

$$\mathrm{PPI} = \frac{I}{I_{\mathrm{opt}}}\exp\left(1-\frac{I}{I_{\mathrm{opt}}}\right) \quad \text{(B18)}$$

$$I = \mathrm{PAR}\cdot\exp\left(k_{\mathrm{w}}z - k_{\mathrm{c}}\int_z^0 \mathrm{d}z'\,\mathrm{Nnorm}(\mathrm{P}+\mathrm{D})\right) \quad \text{(B19)}$$

$$\mathrm{PAR} = \frac{I_0}{2} \quad \text{(B20)}$$

$$I_{\mathrm{opt}} = \max\left(\frac{I_0}{4}, I_{\min}\right) \quad \text{(B21)}$$

$$I_0 = f(t, y, \text{cloudiness}) \quad \text{(B22)}$$

$$\mathrm{LP} = \mathrm{LPN}+\mathrm{LPD} \quad \text{(B23)}$$

B.2.2. Zooplankton rates

$$G_n = \frac{G\cdot\mathrm{P}_n}{\sum_{n=1}^{3}\mathrm{P}_n} \quad \text{(B24)}$$

$$G = G0\cdot\mathrm{TLIMZ}\left(1-\exp\left(-\mathrm{IV}\sum_{n=1}^{3}\mathrm{P}_n^2\right)\right) \quad \text{(B25)}$$

$$\mathrm{TLIMZ} = 1+\frac{\mathrm{e}^2T^2}{T_{\mathrm{optz}}^2\exp\left(\frac{2T}{T_{\mathrm{optz}}}\right)} \quad \text{(B26)}$$

$$\mathrm{LZ} = \mathrm{LZN}+\mathrm{LZD} \quad \text{(B27)}$$

B.2.3. Recycling rates

$$\mathrm{REC} = \mathrm{DN}\left(1+T_{\mathrm{scd}}\frac{T^2}{T_{\mathrm{hsr}}^2+T^2}\right) \quad \text{(B28)}$$

$$\mathrm{RECS} = \begin{cases} \frac{1}{2}\mathrm{DS}\cdot\exp(T_{\mathrm{scs}}T) & : \quad \mathrm{O2}>0 \\ \frac{1}{10}\mathrm{DS}\cdot\exp(T_{\mathrm{scs}}T) & : \quad \mathrm{O2}\le 0 \end{cases} \quad \text{(B29)}$$

$$\mathrm{RECSN} = \begin{cases} \mathrm{RECS} & : \quad \mathrm{O2}>0 \\ 0 & : \quad \mathrm{O2}\le 0 \end{cases} \quad \text{(B30)}$$

B.2.4. Nitrification

$$\mathrm{NF} = \begin{cases} \frac{\mathrm{O2}}{O_{\mathrm{hsn}}+\mathrm{O2}}\cdot\mathrm{TLIMN} & : \quad \mathrm{O2}>0 \\ 0 & : \quad \mathrm{O2}\le 0 \end{cases} \quad \text{(B31)}$$

$$\mathrm{TLIMN} = \mathrm{NI0}\exp(T_{\mathrm{scn}}T) \quad \text{(B32)}$$

B.2.5. Stoichiometric rates

Coupling oxygen sinks and sources to nitrogen transformations stoichiometric relations are used. These rates are based on Redfield ratio:

$$(CH_2O)_{106}(NH_3)_{16}(H_3PO_4)_1$$

Photosynthetic oxygen production could be simplified as:

$$\text{Light} + CO_2 + H_2O \rightarrow CH_2O + O_2$$

The molar ratio of used carbon to produced oxygen equals 1. Using ammonium (NH_3), the Redfield ratio yields:

$$\frac{O_2}{N} = 6.625\left(\frac{\text{produced}\,O_2}{\text{used}\,N}\right)$$

Nitrate (NO_3) supplies 1.5 additional oxygen molecules. Multiplied by Redfield ratio $16/106$, one finds:

$$\frac{O_2}{N} = \frac{106}{16}\left(1 + 1.5\frac{16}{106}\right) = 8.125$$

Under oxic conditions, nitrification occurs.

$$2NH_4 + 3O_2 \rightarrow 2NO_3 - 4H_2$$

$$\frac{N}{O_2} = \frac{2}{3}$$

Remineralisation takes oxygen to reduce organic matter. In the oxic case molecular oxygen,

$$\text{organic nitrogen} \rightarrow \text{anorganic nitrogen (ammonium)}$$

$$(CH_2O)_{106}(NH_3)_{16}H_3PO_4 + 106O_2 \rightarrow 106CO_2 + 16NH_3 + H_3PO_4 + 106H_2O$$

$$\frac{\text{oxygen demand}}{\text{recycled nitrogen}} = \frac{106}{16} = 6.625$$

in the anoxic case (with nitrate present) nitrate,

$$\text{organic N} + \text{nitrate} \rightarrow \text{ammonium and molecular nitrogen}$$

$$(CH_2O)_{106}(NH_3)_{16}H_3PO_4 + 84.4HNO_3 \rightarrow 106CO_2 + 16NH_3 + 42.4N_2 + H_3PO_4 + 148.4H_2O$$

$$\frac{\text{reduced nitrate}}{\text{oxidized detritus}} = \frac{84.8}{16} = 5.3$$

and in the anoxic case without nitrate sulphate,

$$(CH_2O)_{106}(NH_3)_{16}H_3PO_4 + 53H_2SO_4 \rightarrow 106CO_2 + 53H_2S + H_3PO_4 + 106H_2O + 16NH_3$$

$$\frac{\text{synthesized}\,H_2S}{\text{recycled nitrogen}} = \frac{53}{16} = 3.3125$$

is used. Hydrogen sulphide is accounted for as negative oxygen concentrations. To oxidize hydrogen sulphide, 2 mol O_2 are required to oxidize 1 mol H_2S to sulphate. The relation to use negative oxygen concentrations as hydrogen sulphide is:

$$2 \cdot H_2S = 1 \cdot O_2$$

B.3. Switches

$$\text{OSWTCH} = \begin{cases} 1 & : \quad O2 > 0 \\ 0 & : \quad O2 \le 0 \end{cases} \tag{B33}$$

$$\text{NSWTCH} = \begin{cases} 1 & : \quad N > 0 \\ 0 & : \quad N \le 0 \end{cases} \tag{B34}$$

B.4. Surface fluxes

$$\text{OFLX} = \text{PV}(O_{\text{sat}} - O2) \tag{B35}$$

$$O_{\text{sat}} = \frac{31.25}{\text{Onorm}}(14.603 - 0.40215 \cdot T) \tag{B36}$$

B.5. Constants

Parameter	Meaning	Numerical value
α_1	half-saturation diatoms	0.3
α_2	half-saturation flagellates	0.15
α_3	half-saturation blue-greens	0.5
DN	constant scaling mineralisation of detritus	0.003 day^{-1}
DS	constant scaling mineralisation of sediment	0.002 day^{-1}
$G0$	maximum grazing	0.5 day^{-1}
I_{min}	minimum PAR	25 W/m^2
IV	Ivlev constant	1.2
k_w	attenuation constant sea water	0.18 m^{-1}
k_c	attenuation constant self shading	0.03 $m^2/mmol$
LPN	loss rate phytoplankton to nutrients	0.01 day^{-1}
LPD	loss rate phytoplankton to detritus	0.02 day^{-1}
LZN	loss rate zooplankton to nutrients	0.3 day^{-1}
LZD	loss rate zooplankton to detritus	0.6 day^{-1}
NI0	nitrification constant	0.1 day^{-1}
Nnorm	conversion factor model units to N	4.5 $mmol/m^3$
Onorm	conversion factor model units to O_2	375 $mmol/m^3$
PV	piston velocity	5 m/day
O_{hsn}	constant scaling the oxygen dependence of nitrification	0.01
RB0	maximum uptake rate blue-greens	0.5 day^{-1}
RD0	maximum uptake rate diatoms	1 day^{-1}
RES	resuspension rate	25 day^{-1}
RF0	maximum uptake rate flagellates	0.7 day^{-1}
RFR	Redfield ratio P/N	1/16
SEDR	sedimentation rate	3.5 m/day
Ths_2	half-saturation temperature flagellates	10°C
Ths_3	half-saturation temperature blue-greens	16°C
T_{hsr}	constant scaling temperature dependence of detritus mineralisation	13°C
T_{scd}	constant scaling the temperature effect on detritus mineralisation	20
T_{scn}	constant scaling the temperature effect on nitrification	0.11 $°C^{-1}$
T_{scs}	constant scaling the temperature effect on sediment mineralisation	0.15 $°C^{-1}$
T_{optz}	optimum grazing temperature	20°C

References

Bergström, S., Carlsson, B., 1994. River runoff to the Baltic Sea: 1950–1990. Ambio 23, 280–287.

Bock, K.H., 1971. Monatskarten des Salzgehaltes der Ostsee. Dtsch. Hydrogr. Z., 1–147.

Fennel, W., 1995. Model of the yearly cycle of nutrients and plankton in the Baltic Sea. J. Mar. Syst. 6, 313–329.

Fennel, W., Neumann, T., 1996. The mesoscale variability of nutrients and plankton as seen in a coupled model. Ger. J. Hydrogr. 48, 49–71.

Fennel, K., Neumann, T., 1999. Computerized modeling of sedimentary systems, chap. A coupled physical–chemical model for the Western Baltic. 1st edn. Springer-Verlag, Berlin, Heidelberg, pp. 169–182.

Helcom, 1994. Baltic Sea environment proceedings No. 39, Baltic Marine Environment Protection Commission, airborne Pollution Load to the Baltic Sea 1986–1990.

Kayser, W., Schulz, S., 1976. Zur Ursache der zeitlichen und räumlichen Differenz des Beginns der Phytoplantonblüte in der Ostsee. Fischereiforschung 14, 77–81.

Lehmann, A., 1995. A three-dimensional eddy resolving model of the Baltic Sea. Tellus 47A, 1013–1031.

Lenz, W., 1971. Monatskarten der Temperatur der Ostsee. Dtsch. Hydrogr. Z., 1–147.

Losán, J.L., Lampe, R., Matthäus, W., Rachor, E., Rumohr, H., Westernhagen, H.V., 1996. Warnsignale aus der Ostsee. Parey Buchverlag, Berlin.

Mikulski, Z., 1970. Inflow of river water to the Baltic Sea in the period 1951–1960. Nord. Hydrol. 4, 216–227.

Mutzke, A., 1998. Open boundary condition in the GFDL-model with free surface. Ocean, 2–6.

Pacanowski, R.C., Philander, S.G.H., 1981. Parameterization of the vertical mixing in numerical models of the tropic ocean. J. Phys. Oceanogr. 11, 1443–1451.

Pacanowski, R.C., Dixon, K., Rosati, A., 1990. The GFDL Modular Ocean Model Users Guide Version 1.0, GFDL Technical Report No. 2., Geophysical Fluid Dynamic Laboratory, NOAA, Princeton University, Princeton.

Rheinheimer, G., 1996. Meereskunde der Ostsee. Springer-Verlag, Berlin, Heidelberg.

Rosati, A., Miyakoda, K., 1988. A general circulation model for upper ocean simulation. J. Phys. Oceanogr. 18, 1601–1626.

Siegel, H., Bruhn, R., Gerth, M., Nausch, G., Matthäus, W., Neumann, T., Pohl, C., 1998. The exceptional Oder flood in summer 1997 — distribution patterns of the Oder discharge in the Pomeranian Bight. Ger. J. Hydrogr. 50, 145–167.

Stigebrandt, A., Wulff, F., 1987. A model for the dynamics of nutrients and oxygen in the Baltic proper. J. Mar. Res. 45, 729–759.

Wasmund, N., 1997. Occurrence of cyanobacterial blooms in the Baltic Sea in relation to environmental conditions. Int. Rev. Gesamten Hydrobiol. 82, 169–184.